Regular Article

PHYSICAL CHEMISTRY RESEARCH
Published by the
Iranian Chemical Society
www.physchemres.org
info@physchemres.org

Phys. Chem. Res., Vol. 11, No. 2, 299-313, June 2023
DOI: 10.22036/pcr.2022.339408.2087

First-Principles Study on Optoelectronic and Photovoltaic Properties in a P3HT/PCBM Complex

A. El Ghazali[a], A. Aboulouard[b,c], S. Zouitina[a], S. Atlas[d], M. El Idrissi[e,*] and A. Tounsi[a]

[a]*RTACM, Polydisciplinary Faculty, Sultan Moulay Slimane University, Beni-Mellal, Morocco*
[b]*Department of Physics, Sultan Moulay Slimane University, Beni-Mellal, Morocco*
[c]*Department of Engineering Sciences, Izmir Katip Celebi University, Cigli, 35620 Izmir, Turkey*
[d]*Polydisciplinary Faculty, Sultan Moulay Slimane University, Beni-Mellal, Morocco*
[e]*TCPAM, Polydisciplinary Faculty, Sultan Moulay Slimane University, Beni-Mellal, Morocco*
(Received 26 April 2022, Accepted 9 June 2022)

Due to their diverse potentials, solar cells based on conjugated polymers have attracted attention over the past decades. In this study, 10 poly(3-hexylthiophene) (P3HT)-based solar cells were studied by performing computations based on density functional theory (DFT) and time-dependent density-functional theory (TD-DFT) with increasing molecular chains. The effects of the increase in the number of monomers on the optoelectronic properties, including frontier molecular orbitals (FMOs), molecular electrostatic potential (MEP), global reactivity descriptors, dipole moment, charge mobilities, and optical characteristics, were investigated. The results demonstrated that M (n = 3) had a smaller gap energy, best optical properties, and highest charge mobilities. In addition, the photovoltaic characteristics of novel donors were examined using (6,6)-phenyl-C61-butyric acid methyl ester (PCBM), as an electron acceptor. The results showed that compounds M (n = 1) to M (n = 10) had an efficient electron transport from donor to acceptor. These results suggest that these engineered molecules can be tested in the laboratory to improve organic solar cells (OSCs).

Keywords: TD-DFT, Organic photovoltaic cell, FMO, MEP, P3HT, Donor materials

INTRODUCTION

In recent decades, conductive organic polymers have emerged as one of the most promising materials for organic photovoltaic (OPV) devices due to their low manufacturing cost on flexible plastic substrates [1-2]. The OPV research is a highly multidisciplinary field requiring advanced skills in molecular and macromolecular engineering, physicochemistry, and physics of materials. Energy conversion efficiency can be improved by exploring the chemical and physicochemical mechanisms involved in active materials and examining the technological aspects of photovoltaic devices. The benefits of OPV devices outweigh their low power conversion efficiency (PCE), which is attributed to their limited absorption spectra and low charge mobility compared to inorganic materials. Over the last two decades, the development of donor and acceptor materials incorporated into the active layer of organic solar cells (OSCs) has resulted in an almost 8% increase in their PCE [3].

The development of novel organic electron materials is one of the most important areas in the development of enhanced OPVs. A precise balance between the energy levels of the acceptor and donor materials, as well as good absorption and mobility, must be achieved to develop such materials [4]. In the production of polymer-based OSCs, cost-effective techniques most typically utilized include sputtering, spin coating, and printing [5]. because of Due to their good thermal and environmental stability, high

*Corresponding author. E-mail: m.elidrissi2018@gmail.com

electrical conductivity, and corrosion resistance, polythiophene and its derivatives are most frequently utilized as polymers in the manufacturing of low-cost flexible electronics [1-2]. Moreover, polythiophene and its derivatives are not affected by the protonation reaction of polyaniline and exhibit relatively simple electrochemical activity [6].

Novel polymers based on 3-substituted thiophene, particularly poly(3-alkylthiophenes), are the derivatives most investigated as active materials in OPV cells. They have led to significant progress in materials research [7]. The poly(3-hexylthiophene) (P3HT) homopolymer is one of the most promising polymer donor materials with a low cost and a controlled group [8-9]. The photophysical properties of this homopolymer are governed by its regioregularity [10], which can be controlled to produce highly ordered structures with improved photoconversion characteristics and enhanced charge carrier mobility [11]. Although numerous investigations have been carried out on P3HT, the PCE of P3HT-based photovoltaic solar cells is still only 7.4% in fullerene-based binary devices and 7.8% in fullerene-free ternary devices, which is due to the high HOMO energy level and a narrow absorption band [12-19]. There are a variety of approaches that can be employed to correct or mitigate this imbalance. However, as the number of motifs grows, the number of π and π* molecular orbitals grows and the energy gap between HOMO and LUMO decreases. In photodetector devices, the fundamental P3HT/PCBM donor/acceptor combination has been widely used [20-21].

As previously stated, density functional theory (DFT) and time-dependent density functional theory (TD-DFT) are appropriate tools to identify the physical properties of materials based on quantum approximations with various numerical codes [22-23]. DFT and TD-DFT computations are widely used to predict the optoelectronic and photovoltaic properties of materials used in photovoltaic cells [24-27].

The goal of this research was to extend the experimental work on P3HT and PCBM using a rigorous theoretical examination based on DFT and TD-DFT to illustrate precisely the structure-optoelectronic correlation property of these materials. As in many other OSC materials, the heterojunction structure was adopted in the P3HT:PCBM blends, and the number of monomers was increased to increase the donor/acceptor interface.

CALCULATION METHOD AND THEORETICAL METHODOLOGY

The quantum computations were performed with the Gaussian 09 program [28] and visualized by GaussView 5.0.8. The geometric structure of all materials was optimized using DFT at the B3LYP/6-31G(d.p) basis set level [29]. The B3 indicates the three-parameter Becke exchange, and LYP indicates the Lee-Yang-Parr correlational functional [30]. The energy levels of the frontier molecular orbitals (FMOs) were deduced from the results files of the optimized structures. Moreover, the electronic transition energy, absorption maxima, and oscillation strength were calculated using the TD-DFT/B3LYP/6-31(d.p) method.

The electronic affinities and vertical ionization potentials were calculated using Eqs. (1) and (2).

$$IP = [E^+ - E] = E_{HOMO} \quad (1)$$

$$EA = [E_0 - E^-] = E_{LUMO} \quad (2)$$

where IP and EA are the ionization potentials and electronic affinities (eV), respectively, E^+ is the energy in the cationic state in atomic units of energy (a.u), E_0 is the energy in the neutral state (a.u), and E^- is the energy in the anionic state (a.u).

The calculation of the total energy of ionic and neutral systems allowed the researchers to calculate ionization potentials and electron affinities, which, in turn, ensure the efficient migration of electrons and holes [31-32].

FMOs analysis was used to explain the molecular properties of the investigated compounds, researchers use. To elucidate the molecular features of the studied compounds (n = 10), the magnitudes of the FMOs were used to evaluate their chemical hardness, chemical potential, softness, and electrophilicity index, as shown in Eqs. ((3)-(6)):

$$\mu = \frac{(E_{HOMO} + E_{LUMO})}{2} \quad (3)$$

$$\eta = -\frac{(E_{HOMO} - E_{LUMO})}{2} \quad (4)$$

$$S = \frac{1}{2\eta} \quad (5)$$

$$\omega = \frac{\mu^2}{2\eta} \quad (6)$$

where μ, η, S, and ω are the chemical potential, chemical hardness, softness, and electrophilicity index (eV), respectively, and E_{HOMO} and E_{LUMO} are the HOMO and LUMO energy levels of the compounds (eV), respectively.

RESULTS AND DISCUSSION

Structural Properties

Quantum approaches, including DFT and TD-DFT, were used to investigate the structural geometry and electrical behavior of organic molecules in stable and unstable states. Ten compounds that were oligomers of P3HT (from M (n = 1) - M (n = 10)) were theoretically examined to investigate the effect of chain length on spectroscopic and photovoltaic features. The optimized structures of the examined chain length are shown in Fig. 1.

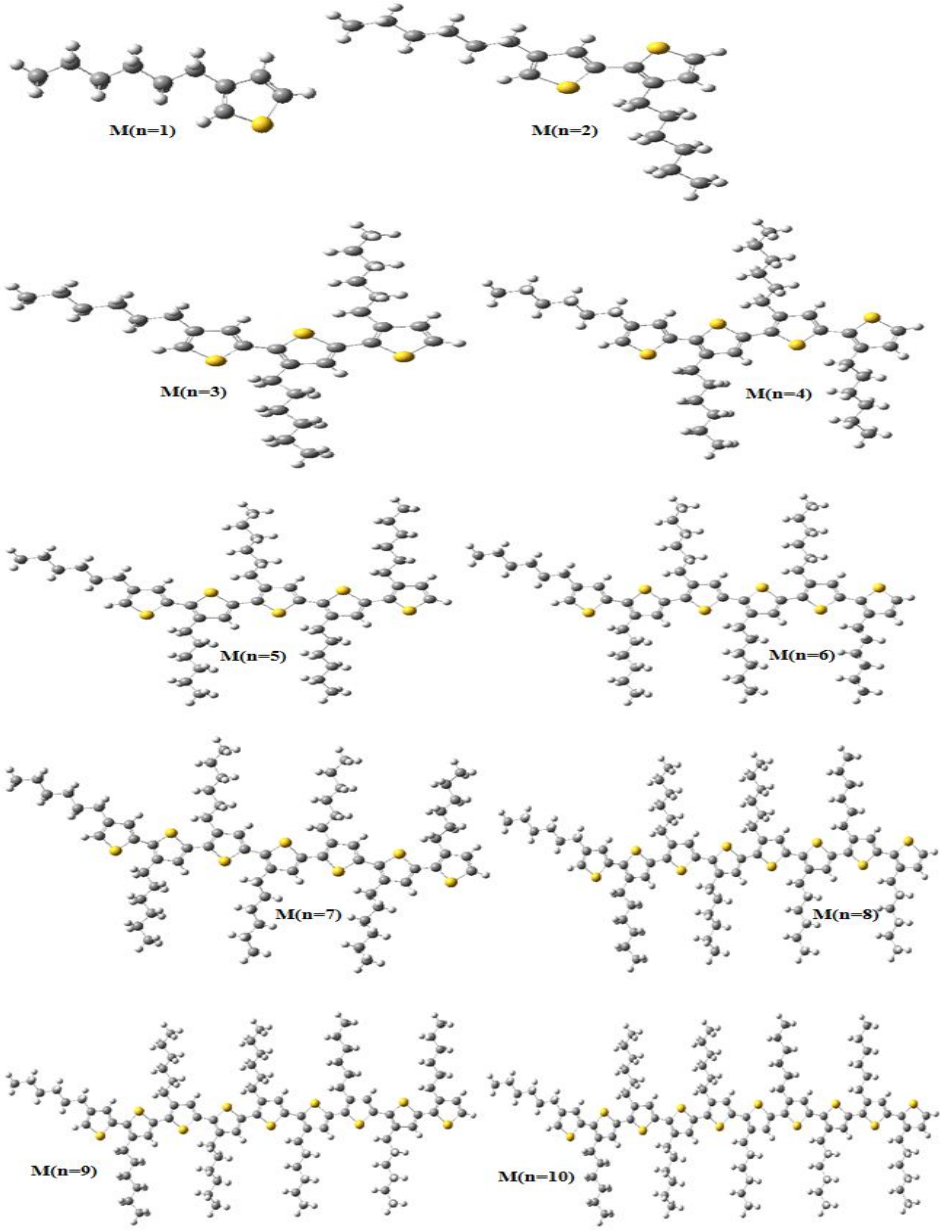

Fig. 1. The optimized structures of the examined compounds M (n = 1-10) using DFT at the 6-31G(d,p) basis set.

Frontier Molecular Orbitals (FMOs)

The FMOs energy levels are crucial to having efficient OSCs. The charge transfer from the donor to the acceptor is affected by the difference between FMOs energy levels, known as the gap energy. As a result, when light is absorbed, molecules with low E_{Gap} allow electron transfer from HOMO to LUMO. Furthermore, due to their simple ionization, π-electrons play a crucial role in conjugated systems. From HOMO (π) to LUMO (π*), electrons may be emitted to the conjugated π-molecule. The quantum approach can be used to determine the positions of these levels. The E_{HOMO}, E_{LUMO}, and E_{Gap} values of the studied molecules are shown in Table 1.

The HOMO and LUMO energy levels of the donor and acceptor compounds are critical in establishing whether a compound is a donor or an acceptor. Furthermore, a compound with a reduced energy gap is more stable than other compounds.

The E_{HOMO} and E_{LUMO} of the 10 studied compounds varied considerably, as can be seen in Table 1. The LUMO energy of the compounds M (n = 1-10) were -2.211, -2.325, -3.049, -3.423, -3.441, -3.459, -3.556, -3.627, -3.629, and -3.658 (eV), respectively while their HOMO energy were -4.028, -4.126, -4.446, -4.887, -4.987, -5.331, -5.411, -5.654, -5.698, and -5.879 (eV), respectively.

The 10 designed compounds had greater LUMO levels than PCBM, as indicated in Table 1. This suggests that these compounds can have good electron injection into PCBM acceptors, implying that they could be useful in solar systems.

Figure 2 presents the HOMO and LUMO orbitals of each of the 10 studied molecules. The central skeleton was distributed on the acceptor part of the LUMO and HOMO of compounds M (n = 1-4). However, in LUMOs, the electron density was distributed among the groups present at the end of the acceptor group. The HOMOs were located on the central unit of the backbone of compounds M (n = 5-8), M (n = 3), and M (n = 10). Moreover, the low electron density was distributed on the groups capped at the acceptor end in LUMOs.

Electronic Properties

Table 1 lists the determined quantum chemical parameters, including the energy gap (E_{Gap}), chemical potential (μ), overall hardness (η), softness (S), and overall electrophilicity (ω). The photovoltaic performance of organic

Table 1. HOMO Energy, LUMO Energy, Band Gap, Chemical Potential, Overall Hardness, Softness, and Overall Electrophile Index Calculated at the B3LYB/6-31G(d,p) level for the Ten Studied Compounds

Compounds	E_{HOMO} (eV)	E_{LUMO} (eV)	E_{Gap} (eV)	μ (eV)	η (eV)	S (eV)
M (n = 1)	-4.028	-2.211	1.817	-3.119	0.908	0.550
M (n = 2)	-4.126	-2.325	1.801	-3.225	0.9	0.555
M (n = 3)	-4.446	-3.049	1.397	-3.747	0.698	0.716
M (n = 4)	-4.887	-3.423	1.464	-4.155	0.732	0.683
M (n = 5)	-4.987	-3.441	1.546	-4.214	0.773	0.646
M (n = 6)	-5.331	-3.459	1.872	-4.395	0.936	0.534
M (n = 7)	-5.411	-3.556	1.855	-4.483	0.927	0.539
M (n = 8)	-5.654	-3.627	2.027	-4.640	1.013	0.493
M (n = 9)	-5.698	-3.629	2.069	-4.663	1.034	0.483
M (n = 10)	-5.879	-3.658	2.221	-4.768	1.110	0.450
PCBM	-6.110	-3.711	2.399	-4.910	1.199	0.417

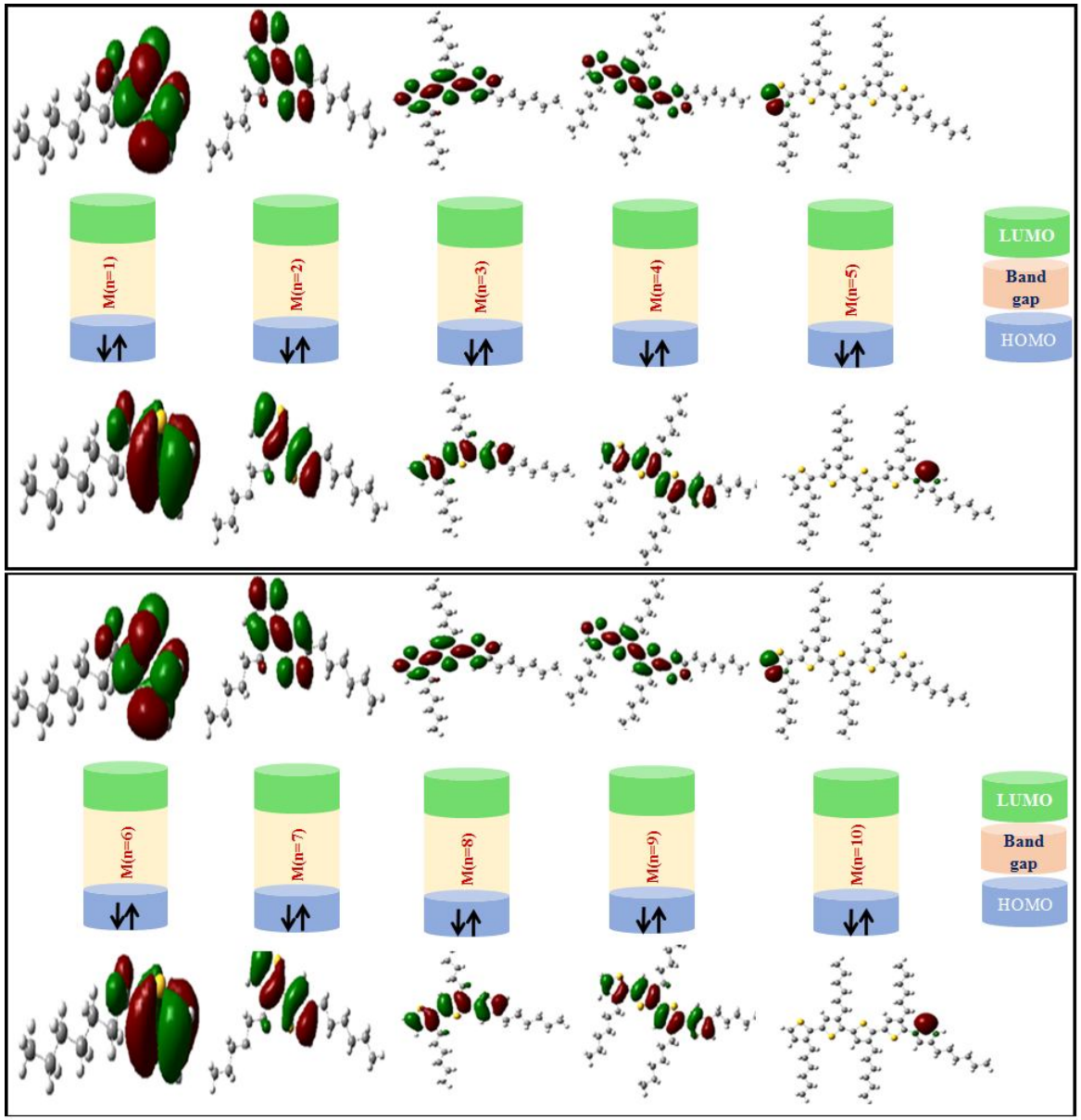

Fig. 2. The contour curves of the HOMO and LUMO orbitals of the investigated compounds.

solar cells was influenced by the E_{LUMO}, E_{HOMO}, and E_{Gap} of FMOs, which were used to determine the open-circuit voltage (V_{oc}). Open-circuit voltage, in turn, was used to evaluate electron transport properties, dynamic stability, chemical hardness, and chemical reactivity [33].

As shown in Table 1, E_{Gap} varied from -2.221 to -1.817 (eV). Among all the studied compounds, M (n = 3) had the lowest E_{Gap} value, indicating that this compound had the most stabilized HOMO and LUMO. Overall, the gap energy decreased in the following order: M (n = 10) > M (n = 9) > M (n = 8) > M (n = 6) > M (n = 7) > M (n = 1) > M (n = 2) > M (n = 5) > M (n = 4) > M (n = 3).

The ability of a system to exchange electron density with its surrounding is measured by chemical potential. As shown in Table 1, the chemical potential of the 10 studied compounds was higher than that of PCBM, which is

extensively employed as an acceptor in organic solar cells. The compounds showed different chemical potentials based on the following descending order: M (n = 1) > M (n = 2) > M (n = 3) > M (n = 4)) > M (n = 5) > M (n = 6) > M (n = 7) > M (n = 8) > M (n = 9) > M (n = 10) > PCBM. Table 1 shows that the investigated compounds had high chemical potentials, implying that they can act as electron donors and that the PCBM can function as an electron acceptor in bulk-heterojunction (BHJ) solar cells due to electron transfer from the higher to lower chemical potential**.**

Generally, organic molecules are divided into two types: hard and soft molecules. Hard molecules are characterized by a high energy gap while soft molecules are characterized by a low energy gap.

Figure 3 demonstrates that the studied compounds had low chemical hardness but high softness. It, therefore, can be concluded that they are soft molecules, which can be explained by their low E_{Gap}. Moreover, Fig. 3 shows that compound M (n = 3) was the softest and hardest, which renders it a very promising compound for OSC devices.The energy was supplied when an extra electron was acquired from the environment, which is reflected in the global electrophilicity index. Table 1 shows that as the number of M units increased, the electrophilicity index increased, too. The low electrophilicity index of the compounds indicated that electrons were attracted to the PCBM. Furthermore, PCBM was more electrophilic than the studied compounds, implying that the studied compounds can be used as electron donors. Thus, it can be stated that while PCBM will act as an electron acceptor in OSC devices, the studied compounds will serve as potential donors.

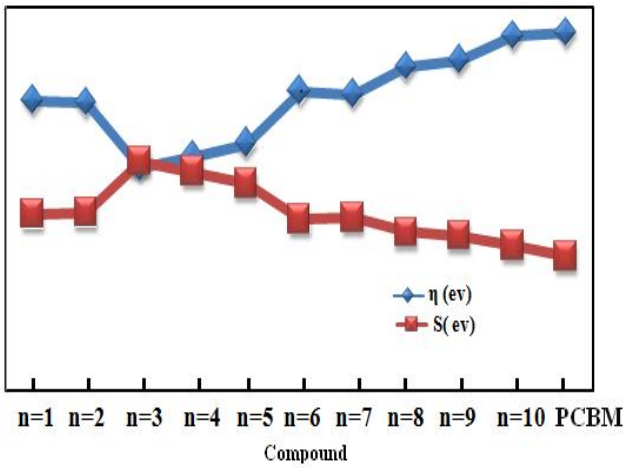

Fig. 3. The hardness and softness of the examined compounds.

Table 2. HOMO Energy, LUMO Energy, and Open Circuit Voltage of the Ten Investigated Compounds

Compounds	E_{HOMO} (eV)	E_{LUMO} (eV)	V_{oc} (V)
M (n = 1)	-4.028	-2.211	1.517
M (n = 2)	-4.126	-2.325	1.501
M (n = 3)	-4.446	-3.049	1.097
M (n = 4)	-4.887	-3.423	1.164
M (n = 5)	-4.987	-3.441	1.246
M (n = 6)	-5.331	-3.459	1.572
M (n = 7)	-5.411	-3.556	1.555
M (n = 8)	-5.654	-3.627	1.727
M (n = 9)	-5.698	-3.629	1.769
M (n = 10)	-5.879	-3.658	1.921

Photovoltaic Properties

The photovoltaic characteristics of the examined compounds were determined. The difference between the energy level of a donor and that of an acceptor represents the open-circuit voltage (V_{oc}) [34].

The theoretical V_{oc} values were determined using Eq. (7) [35]:

$$V_{OC} = \frac{1}{e}\left(\left|E_{HOMO}\,(\text{Donor})\right| - \left|E_{LUMO}\,(\text{Acceptor})\right| - 0{,}3\right) \quad (7)$$

where V_{oc} is the open-circuit voltage (V), e is the elemental charge, E_{HOMO} (donor) is the HOMO energy of the compounds (eV), E_{LUMO} (acceptor) is the LUMO energy of the acceptor (eV), and 0.3 is an empirical factor representing the typical loss contained in the BHJ.

Table 2 shows that the HOMO and LUMO energy levels of the studied compounds were greater than those of PCBM, facilitating an effective electron injection into PCBM.

The obtained V_{oc} values for all analyzed compounds were in the range of 1.097 V to 1.921 V, which were sufficient for electron transport from donor to acceptor, as shown in Table 2 and Fig. 4.

The value of V_{oc} for the studied compounds is presented below in an ascending order: M (n = 3) < M (n = 4) < M (n = 5) < M (n = 2) < M (n = 1) < M (n = 7) < M (n = 6) < M (n = 8) < M (n = 9) < M (n = 10). Compound M (n = 10) had a high V_{oc} value, implying that it had a high charge conductivity.

Molecular Electrostatic Potential (MEP)

The MEP was computed using the B3LYP/6-31G(d,p) level. The MEP is an important tool to investigate molecular interactions in a specific compound. In addition, the MEP can be used to interpret sites of relative reactivity for electrophilic and nucleophilic attacks, hydrogen bonding interactions, studies of zeolites, molecular cluster and crystal behavior,biological recognition studies, and prediction of a wide range of macroscopic properties [36-38].

The electrostatic potentials on the surface of the studied compounds are depicted in different colors in Fig. 5. Negative electrostatic potential is represented by red color, positive electrostatic potential by blue color, and zero potential by green color. In addition, the negative MEPs (red color) corresponded to electrophilic reactivity whereas the positive MEPs (blue color) referred to nucleophilic reactivity. The colors red, orange, yellow, green, and blue show increased potential. It should be noted that all compounds had significant charge separation. It can be inferred from the previous discussion that the novel compounds under investigation had efficient charge carrier characteristics.

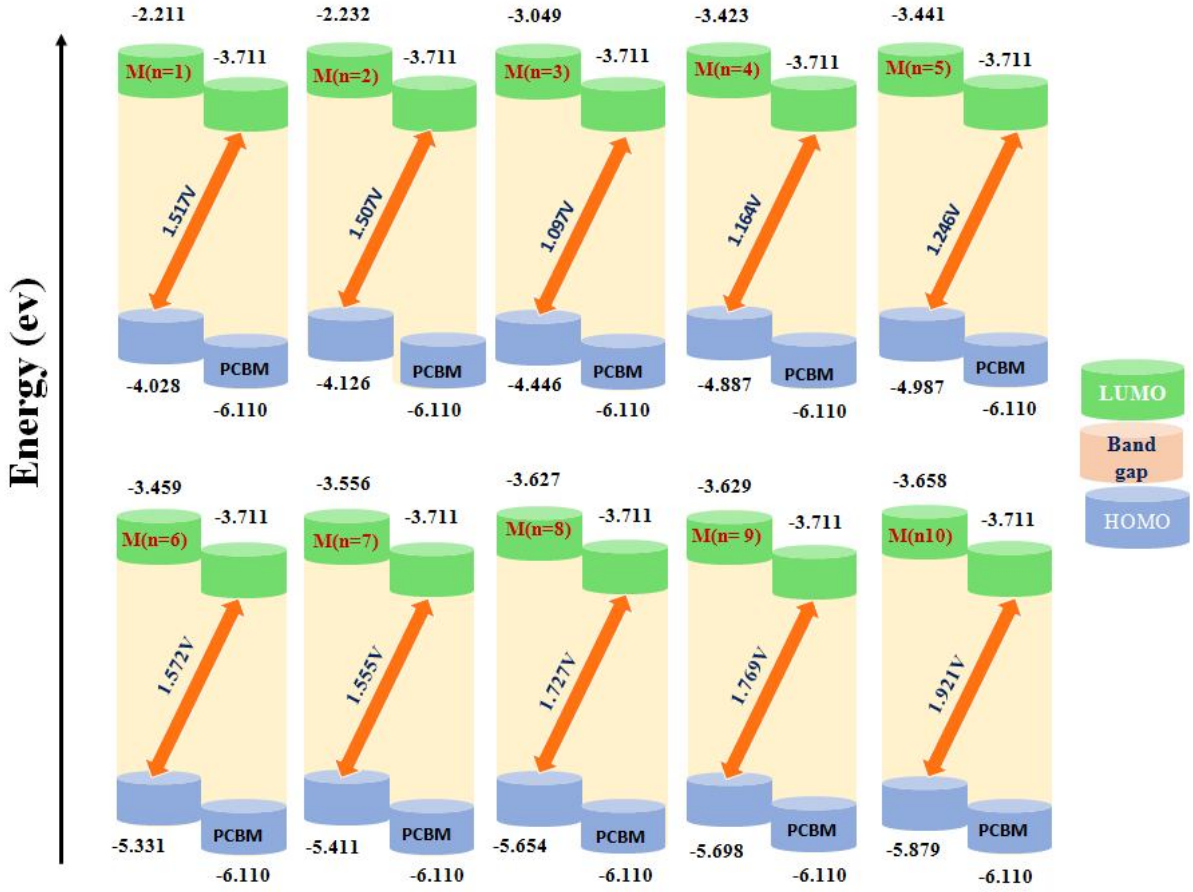

Fig. 4. The open-circuit voltage of all investigated compounds at the B3LYP/6-31G(d,p) level.

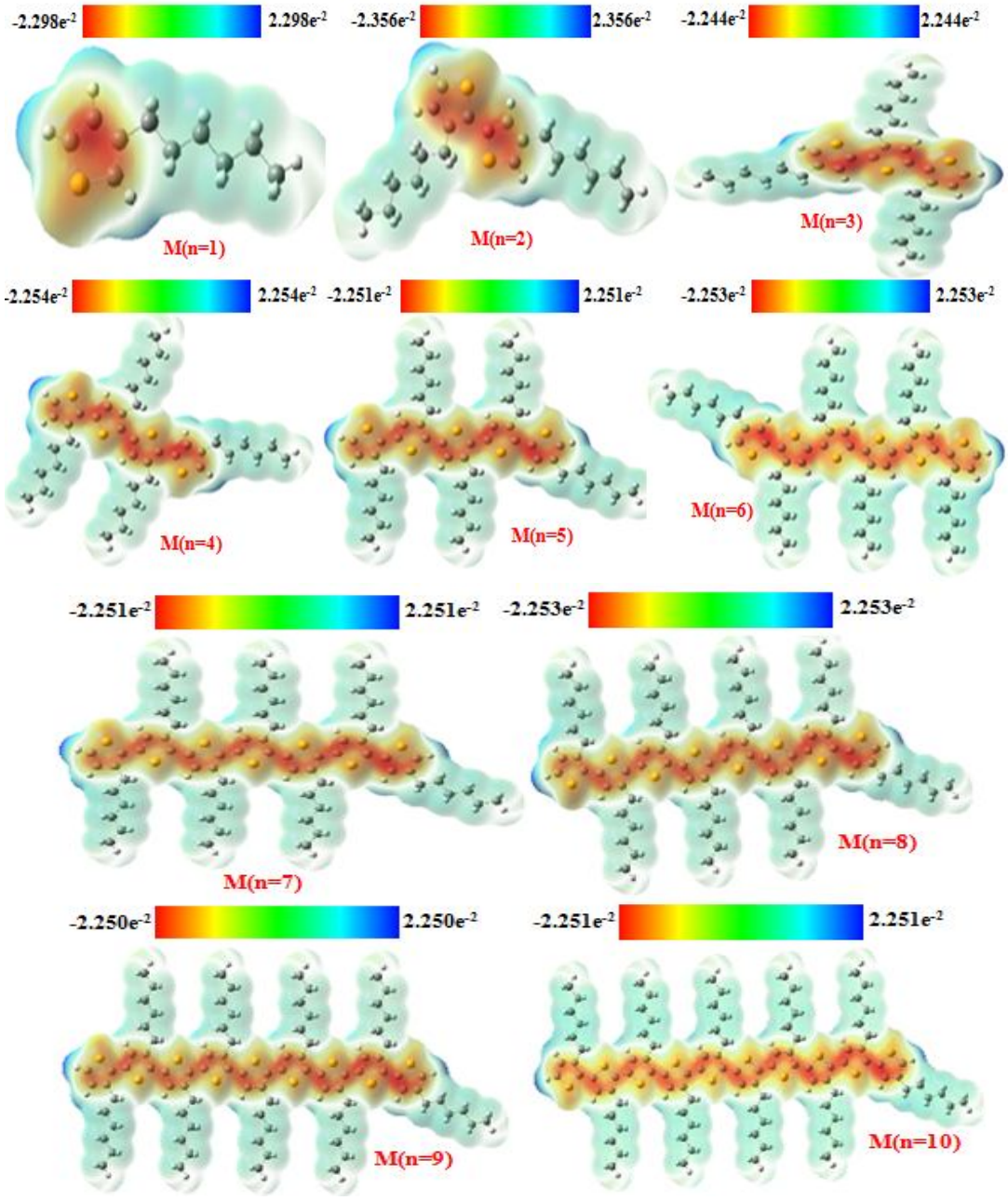

Fig. 5. The MEP of the studied compounds obtained at the B3LYP/6-31G(d,p) level.

UV-Vis Absorption Properties

The absorption of the studied compounds in the visible spectrum was considered critical in defining their optimal photovoltaic performance [39]. The optimized structures were used to determine the UV-Vis absorption spectra of the examined compounds at the TD-DFT B3LYP/6-31G(d,p) level. Figure 6 illustrates the simulated UV-Vis absorption spectra of all examined compounds.

All the 10 studied compounds had maximum absorbance values (λ_{max}) between 203.93 and 438.65 nm. As the chain length increased, an absorption band appeared that shifted toward longer wavelengths (lower energy). This effect is

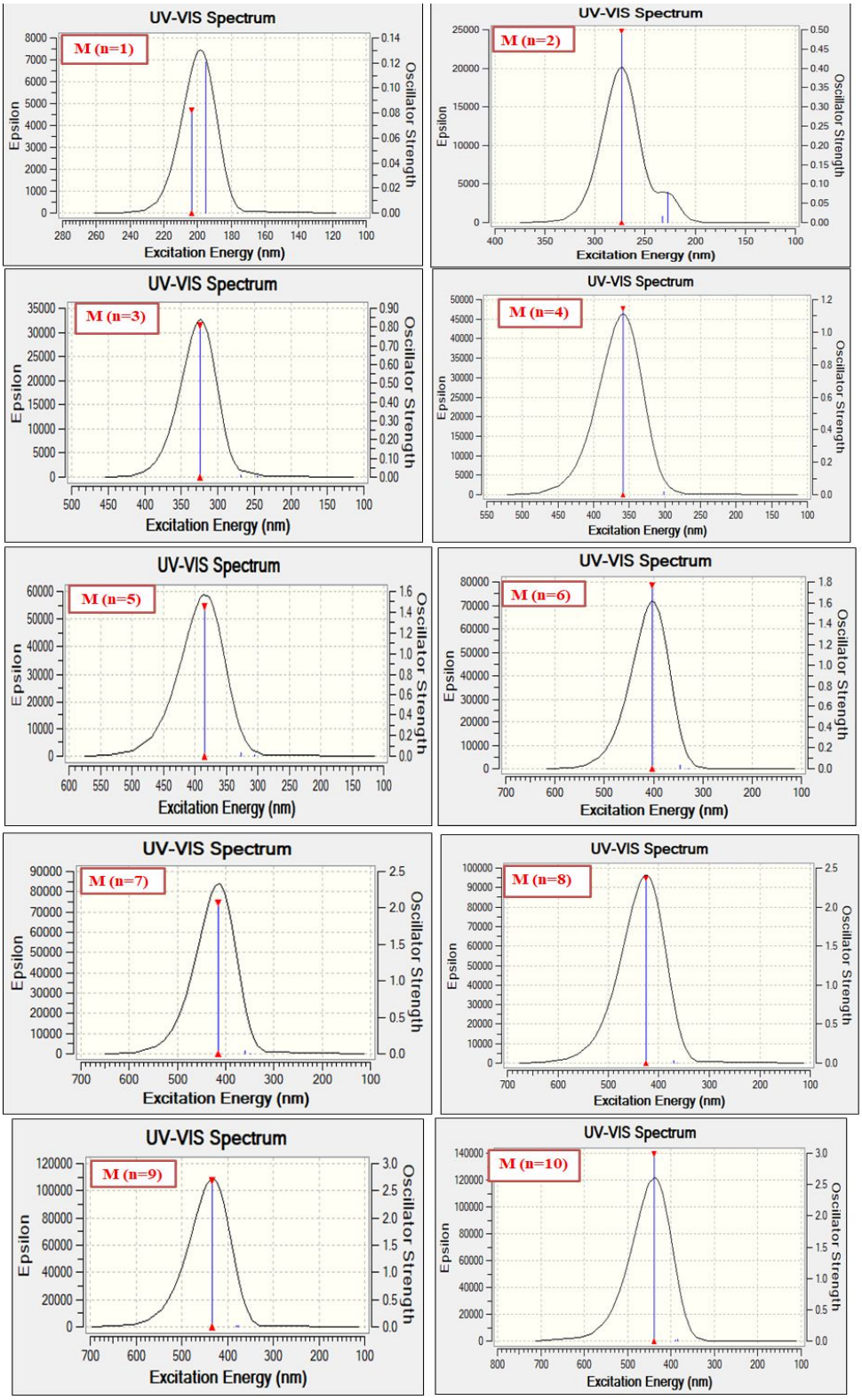

Fig. 6. The simulated UV-Vis absorption of all studied compounds at the B3LYP/6-31G(d,p) level.

most commonly seen in π-conjugated oligomers and is due to the lengthening of conjugation as the number of monomers grows. In this study, it was observed that as the (*n)* increased from 1 to 10, the absorption maximum increased, too. As a result, all compounds (n = 1-10) had exceptional optical characteristics, making them suitable candidates for OSC devices.

Non-Linear Optics

Dipole moments (DM) and the first- and second-order hyperpolarizability values [40] were estimated using the B3LYP/6-31G(d,p) level of DFT [41]. These proprieties had a significant impact on intermolecular interactions (Table 4). Molecular complexity can be related to the polarizability anisotropy (Δα) [30,40-44]. The higher is the anisotropic value of α, the more complicated is the structure of the compound (Δα). DM is a measure of α of a molecule in its ground state, and α is a measure of the intrinsic ability of a molecule to have a dipole in the external electric field. The static electric field (force F) and the total energy (E) of a molecule can be expressed as a Taylor series using Equation (8).

$$E_F = E_0 - \mu_\alpha F_\alpha - \frac{1}{2!}\alpha_{\alpha\beta}F_\alpha F_\beta - \frac{1}{3!}\alpha_{\alpha\beta\Upsilon}F_\alpha F_\beta F_\Upsilon - \frac{1}{4!}\alpha_{\alpha\beta\Upsilon\delta}F_\alpha F_\beta F_\Upsilon F_\delta \quad (8)$$

where E_0 denotes the energy of the molecule in the absence of an external electric field. The molecule properties include energy (E_0), dipole moment (μ_α), polarizability ($\alpha_{\alpha\beta}$), and first- and second-order hyperpolarizability ($\beta_{\alpha\beta\gamma}$ and $\gamma_{\alpha\beta\gamma\delta}$, respectively). First- and second-order hyperpolarizabilities are expressed as tensor quantities while the abbreviations single, double, and so on denote the first- and second-order tensors in Cartesian coordinates [45].

The components of the induced moment will be parallel to the external field if it is located on one of the three orthogonal Cartesian axes. In such a case, the off-diagonal terms of the tensor disappear. The following equation can be used to calculate the expected value of DM under the given conditions:

$$DM = \sqrt{(\mu^2_X + \mu^2_Y + \mu^2_Z} \text{ or} < \alpha_{Static} > = \frac{1}{3}(\alpha_{xx} + \alpha_{yy} + \alpha_{zz}) \quad (9)$$

In the case of the anisotropic orientation of the external field, the polarizability anisotropy (<Δα>) can be calculated as follows:

$$\langle\Delta\alpha\rangle = \left[\frac{(\alpha_{xx} - \alpha_{yy})^2 + (\alpha_{yy} - \alpha_{zz})^2 + (\alpha_{yy} - \alpha_{zz})^2 + 6(\alpha^2_{xy} + \alpha^2_{xz} + \alpha^2_{yz})}{2}\right]$$

Similarly, the first-order ($\beta_{\alpha\beta\gamma}$) and second-order ($\gamma_{\alpha\beta\gamma\delta}$) hyperpolarizability values were calculated from the components of the respective tensors obtained from the Gaussian 09 output file.

$$\beta_i = \beta_{iii} + \frac{1}{3}\sum_{i\neq k}(\beta_{ikk} + \beta_{kik} + \beta_{kki}) \quad (11)$$

$$< \beta_{Static} >= [\beta^2_x + \beta^2_v + \beta^2_z]^{\frac{1}{2}} \quad (12)$$

$$<\beta static> = [(\beta_{xxx} + \beta_{xyy} + \beta_{xzz})^2 + (\beta_{yyy} + \beta_{yzz} + \beta_{vxx})^2 + (\beta_{zzz} + \beta_{zxx} + \beta_{zvv})^2]^{\frac{1}{2}} \quad (13)$$

$$\langle\gamma_{static}\rangle = \frac{\gamma_{xxxx} + \gamma_{yyyy} + \gamma_{zzzz} + 2\gamma_{yyyx} + 2\gamma_{yyzz} + }{5} \quad (14)$$

To ensure higher accuracy, all of the above optical terms were calculated using a set of appropriate bases that included polarized and scattered functions with the DFT/B3LYP/6-31G(d,p) basis set. Tables 3, 4, and 5 present the electric

Table 3. Cartesian Components and Net Electric Dipole Moments (DM in Debye) of the Studied Compounds

Compounds	DMx	DMy	DMz	DM $_{Total}$
M (n = 1)	-0.806	0.297	0.000	0.859
M (n = 2)	0.129	-0.416	-0.000	0.436
M (n = 3)	0.681	-0.990	0.000	1.202
M (n = 4)	-0.332	-0.368	-0.000	0.496
M (n = 5)	0.422	-1.122	0.001	1.199
M (n = 6)	0.391	-0.253	0.0005	0.466
M (n = 7)	0.373	-1.119	0.0012	1.179
M(n = 8)	0.347	0.214	-0.0006	0.408
M (n = 9)	0.3088	-1.1150	0.0014	1.157
M (n = 10)	0.279	0.199	-0.0019	0.343

Table 4. The Optimized Polarizability of the Ten Studied Compounds Calculated by the DFT/B3LYP/6-31G Method

	M (n = 1)	M (n = 2)	M (n = 3)	M (n = 4)	M (n = 5)	M (n = 6)	M (n = 7)	M (n = 8)	M (n = 9)	M (n = 10)
αxx	-82.935	-139.352	-213.194	-275.794	-350.114	-415.307	-487.734	-554.092	-625.128	-692.045
αxy	1.688	-1.156	2.936	-2.465	1.853	10.488	2.354	-15.935	3.0079	-20.737
αyy	-80.665	-147.072	-217.488	-294.197	-361.166	-435.564	-504.006	-577.336	-646.924	-719.728
αxz	0.005	-0.003	0.004	-0.027	0.013	-0.048	0.015	0.038	0.017	0.090
αyz	-0.004	0.012	0.004	0.005	-0.017	-0.026	-0.030	-0.022	-0.049	-0.078
<α>	82.374	51.020	219.863	291.476	363.748	435.455	507.588	579.327	651.378	723.128

Table 5. The Optimized First-Order Hyperpolarizability Calculated by the B3LYP/6-31G Method

	M (n = 1)	M (n = 2)	M (n = 3)	M (n = 4)	M (n = 5)	M (n = 6)	M (n = 7)	M (n = 8)	M (n = 9)	M (n = 10)
βxxx	48.583	-2.453	-41.218	36.069	-48.135	-26.286	-2.017	39.177	77.360	135.465
βyxx	12.131	34.650	-34.970	34.652	-84.838	-5.048	-187.074	34.693	-324.67	63.109
βyyz	-0.010	-0.012	-0.038	0.026	0.016	-0.106	-0.048	0.028	-0.091	0.033
βxyz	-0.019	0.049	-0.012	-0.027	-0.007	0.0321	-0.004	0.229	0.0141	0.409
βzxx	-0.062	-0.105	-0.054	-0.103	0.021	0.1838	0.119	-0.436	0.315	-0.860
βyyy	4.656	22.934	5.836	-2.988	1.759	10.248	1.829	-17.591	2.305	-20.913
βzzz	0.054	0.037	0.039	0.014	0.027	-0.005	0.069	0.064	0.106	0.066
βxzz	-13.468	4.365	14.121	-11.888	17.213	18.406	21.226	22.953	25.265	27.138
βyzz	-3.186	-10.979	-1.862	-10.641	-5.157	-7.291	-5.117	5.993	-5.015	5.422
βxyy	4.649	-13.274	-1.663	-14.276	27.786	40.482	42.345	51.027	54.763	60.664
β_{Tot}	42.025	47.991	42.283	23.239	88.291	32.669	200.066	115.472	363.236	228.289

dipole moment (D), polarizability (α), and hyperpolarizability (β_{total}) of all compounds.

The dipole moment is a crucial parameter in the production of OSCs since it determines the solubility of a compound in a solvent. Organic solvents can quickly dissolve compounds having a high dipole moment value. Table 4 presents the calculated dipole moment values of all studied compounds using the DFT-B3LYP method at the 6-31G(d,p) level. The investigated compounds had a large dipole moment. The dipole moment decreased in the following order: M (n = 3) > M (n = 5) > M (n = 6) > M (n = 7) > M (n = 8) > M (n = 9) > M (n = 10) > M (n = 2) > M (n = 4) > M (n = 1). The dipole moment along the z-axis was zero for all compounds, suggesting that the external field lay on the z-axis of the compounds, as shown in Fig. 1S. Compound M (n = 3) had the highest dipole moment value, which stimulated its self-assembly and provided a strong path for charge transport.

The polarizability, as shown in Fig. 2S and Table 4, decreased in the following order: M (n = 10) > M (n = 9) > M (n = 8) > M (n = 7) > M (n = 6) > M (n = 7) > M (n = 6) > M (n = 5) > M (n = 4) > M (n = 3) > M (n = 2). The maximum polarizability value was observed in compound M (n = 10). The polarizability and the length of the molecular chain were inversely correlated, *i.e.*, the polarizability fell as the chain length grew. Hyperpolarizability (β) was correlated with intramolecular charge transfer (ICT), causing electron flow from the donor group to the acceptor group via the π-conjugation. As can be seen in Fig. 2S and Table 5, the first-order hyperpolarizability decreased in the following order: M

(n = 9) > M (n = 10) > M (n = 7) > M (n = 8) > M (n = 5) > M (n = 2) > M (n = 3) > M (n = 1) > M (n = 6) > M (n = 4), showing that compound M (n = 9) had the highest first-order hyperpolarizability value. The high values of the optimized parameters suggest that the investigated compounds are promising candidates for high-performance nonlinear optical materials.

Mulliken charges were used to calculate the charges of each atom in a compound. The distribution of positive and negative charges plays a critical role in increasing or decreasing the bond length between atoms. Furthermore, the distribution of charges on atoms supports the development of donor and acceptor pairs in the molecule that involves charge transfer [46-47]. Due to the atomic charges, dipole moments, molecular polarizability, electronic structure, acid-base behavior, and several other features of molecular systems, efficient atomic calculations are essential in computing the chemical properties of molecular systems. The Mulliken charges were used to compute the charge distribution of the studied compounds using the B3LYP/6-31G(d,p) level of theory. The values of Mulliken atomic charges are shown in Table 1S, which indicates that the Mulliken charges of the studied compounds increased as the chain length increased.

Natural bond orbital (NBO) population analysis is an efficient technique to study intra- and intermolecular bonds and interactions; it also provides a useful basis to study charge transfer or the conjugational interaction in molecular systems.

The charge distribution in different sub-shells, including core, valence, and Rydberg, of the molecular orbital was clearly described by performing the NBO population analysis on all studied compounds. Table 2S shows the accumulation of natural charges on each atom of these 10 compounds. Table 3S shows that the electron populations of atoms were accumulated in the core, valence, and Rydberg orbitals of the studied compounds.

The following observations can be made based on the examination of Fig. 3S:

- The NBO and Mulliken charges changed as a result of the chain extension;
- Although both the NBO and Mulliken charges increased, the Mulliken charges increased faster than the NBO charges;
- According to the Mulliken and NBO charge values, sulfur had the largest positive charge. Furthermore, the partial charge values were consistent with the electronegativity (χ) of each atom, which evolved as follows: $\chi_C > \chi_S$. This shows that the computed charges were in agreement with the variation in the predicted physicochemical properties.

CONCLUSIONS

In this work, a complete theoretical investigation was conducted to study the electronic, optical, and photovoltaic properties of 10 P3HTcompounds by increasing the number of monomers and using DFT/TD-DFT at the 6-31G(d,p) basis set. In particular, the increase in the number of units allowed more effective modulation and modification of electrical, optical, and photovoltaic properties of the studied molecules. The NBO, NLO, FMO, Mulliken charges, MEP, global reactivity descriptors, dipole moment, charge mobilities, and optical characteristics of the modified compounds were examined. The results showed that all the studied compounds had small band gaps, good optical characteristics, and strong charge mobilities. Based on the open-circuit voltage results, the compounds can be identified as suitable candidates for photovoltaic cell applications. The examined compounds showed good photovoltaic characteristics, including an enhanced charge conduction capacity and effective electron transport from donor to acceptor. The findings are quite promising in showing that the studied compounds have the potential to be practically applied to improve the performance of OSC devices.

REFERENCES

[1] Khan, M. U.; Mehboob, M. Y.; Hussain, R.; Fatima, R.; Tahir, M. S.; Khalid, M.; Braga, A. A. C., Molecular Designing of High-performance 3D Star-shaped Electron Acceptors Containing a Truxene Core for Nonfullerene Organic Solar Cells. *J. Phys. Org. Chem.,* **2021**, *34*(1), 1-17, DOI: 10.1002/poc.4119.

[2] Cui, Y.; Yao, H.; Zhang, J.; Xian, K.; Zhang, T.; Hong, L.; Wang, Y.; Xu, Y.; Ma, K.; An, C.; He, C., Wei, Z.; Gao; F.; Hou, J., Single-Junction Organic Photovoltaic Cells with Approaching 18% Efficiency. *J. Adv. Mat.*, **2020**, *32*(19), 1-7, DOI: 10.1002/adma.201908205.

[3] Zhang, Q.; Kan, B.; Liu, F.; Long, G.; Wan, X.; Chen, X.; Zuo, Y.; Ni, W.; Zhang, H.; Li, M.; *et al.*, A Series

Oligothiophenes for Solution-processed Solar Cells with High Efficiency. *J. A.C.S.*, **2014**, *9*, 35-41, DOI: 10.1038/nphoton.2014.269.

[4] Ni, W.; Wan, X.; Li, M.; Wang, Y.; Chen, Y., A-D-A Small Molecules for Solution-Processed Organic Photovoltaic Cells. *J. Chem. Com*., **2015**, *51*(24), 4936-4950, DOI: 10.1039/C4CC09758K.

[5] [5] Aboulouard, A.; Gürek, A.G.; El idrissi, M., Computational Study of Organic Small Molecules Based on Imidazolinone for Photovoltaic Applications. J.Energy. Sources, Part ARecover. *Util. Environ. Eff.*, **2020**, Vol. ? 1-12, DOI: 10.1080/15567036.2020.1827092.

[6] Silva, A. C. D.; Moura Filho, F.; Alves, M. R.; de Menezes, A. J.; Silva M. C., Hybrid Organic Semiconductors from P3HT and Cellulose Nanocrystals Modified with 3-Thiopheneacetic Acid. *J. Synth. Met*, **2021**, *278*, 116804, DOI: 10.1016/j.synthmet.2021.116804.

[7] Xiao, G.; Guo, Y.; Lin, Y.; Ma, X.; Su, Z.; Wang, Q., Controlled Evaporative Self-Assembly of Poly(3-Hexylthiophene) Monitored with Confocal Polarized Raman Spectroscopy. *J. P.C.C.P*, **2012**, *14*, 16286-16293, DOI: 10.1039/C2CP43435K.

[8] Wadsworth, A.; Hamid, Z.; Bidwell, M.; Ashraf, R. S.; Khan, J. I.; Anjum, D. H. C.; J., Cendra Yan; Rezasoltani, E.; Guilbert, A. A. Y.; Azzouzi, M.; Gasparini, N.; Bannock, J. H.; Baran, D.; Wu, H. B.; de Mello, J. C.; Brabec, C. J.; Salleo, A.; Nelson, J.; Laquai; F.; McCulloch, I., Progress in Poly(3-hexylthiophene) Organic Solar Cells and the Influence of its Molecular Weight on Device Performance. *J. Adv. Energy Mater.*, **2018**, *8*, 1801001, DOI: 10.1002/aenm.201801001.

[9] Li, X. J.; Pan, F.; Sun, C. K.; Zhang, M.; Wang, Z. W.; Du, J. Q.; Wang, J.; Xiao, M.; Xue, L. W.; Zhang, Z. G.; Zhang, C. F.; Liu, F.; Li, Y. F., Simplified Synthetic Routes for Low Cost and High Photovoltaic Performance n-type Organic Semiconductor Acceptors. *J. Nat. Commun*, **2019**, *10*, 519, DOI: 10.1038/s41467-019-08508-3.

[10] Chandrasekaran, N.; Kumar, A.; Thomsen, L.; Kabra, D.; McNeill, C. R., High Performance as-cast P3HT: PCBM Devices: Understanding the Role of Molecular Weight in High Regioregularity P3HT. *J. Adv. Mater*, **2021**, *2*(6), 2045-2054, DOI: 10.1039/D0MA00738B.

[11] Takizawa, Y.; Shimomura, T.; Miura, T., Simulation Study of the Initial Crystallization Processes of Poly(3-Hexylthiophene) in Solution: Ordering Dynamics of Main Chains and Side Chains. *J. Phys. Chem.*, **2013**, *117*, 6282-6289, DOI: 10.1021/jp400308b.

[12] Kroon, R.; Lenes, M.; Hummelen, J. C.; Blom, P. W.; De Boer, B., Small Bandgap Polymers for Organic Solar Cells (Polymer Material Development in the Last 5 Years). *J. Polym. Rev*., **2008**, *48*(3), 531-582, DOI: 10.1080/15583720802231833.

[13] Holliday, S.; Ashraf, R. S.; Wadsworth, A.; Baran, D.; Yousaf, S. A.; Nielsen, C. B.; McCulloch, I., High-Efficiency and Air-Stable P3HT-Based Polymer Solar Cells with a New Non-fullerene Acceptor. *J. Nat. Commun.*, **2016**, *7*(1), 1-11, DOI: 10.1038/ ncomms11585.

[14] Zhao, G.; He, Y.; Li, Y., 6.5% Efficiency of Polymer Solar Cells Based on Poly(3-hexylthiophene) and Indene-C60 Bisadduct by Device Optimization. *J. Adv. Mater.*, **2010**, *22*(39), 4355-4358, DOI: 10.1002/adma.201001339.

[15] Guo, X.; Cui, C.; Zhang, M.; Huo, L.; Huang, Y.; Hou, J.; and Li, Y., High Efficiency Polymer Solar Cells Based on Poly(3-Hexylthiophene)/Indene-C 70 Bisadduct with Solvent Additive. *J. Energy Environ. Sci.*, **2012**, *5*(7), 7943-7949, DOI: 10.1039/C2EE21481D.

[16] Baran, D.; Ashraf, R. S.; Hanifi, D. A.; Abdelsamie, M.; Gasparini, N.; Röhr, J. A.; McCulloch, I., Reducing the Efficiency-Stability-Cost Gap of Organic Photovoltaics with Highly Efficient and Stable Small Molecule Acceptor Ternary Solar Cells. *J. Nat. Mater*, **2017**, *16*(3), 363-369, DOI: 10.1038/nmat4797.

[17] Xiao, B.; Tang, A.; Cheng, L.; Zhang, J.; Wei, Z.; Zeng, Q.; Zhou, E., Non-Fullerene Acceptors with A2 = A1-D-A1 = A2 Skeleton Containing Benzothiadiazole and Thiazolidine-2, 4-Dione for High-Performance P3HT-Based Organic Solar Cells. *J. Sol. RRL*, **2017**, *1*(11), 1700166, DOI: 10.1002/solr.201700166.

[18] Huang, H.; Xiao, B.; Huang, C.; Zhang, J.; Liu, S.; Fu, N.; Huang, W., Enhanced Open Circuit Voltage of Small Molecule Acceptors Containing Angular-Shaped

Indacenodithiophene Units for P3HT-Based Organic Solar Cells. *J. Mater. Chem.*, **2018**, C, *6*(45), 12347-12354, DOI: 10.1039/C8TC04608E.

[19] Xiao, B.; Tang, A.; Zhang, Q.; Li, G.; Wang, X.; Zhou, E., A2-A1-D-A1-A2 Type Non-fullerene Acceptors with 2-(1,1-dicyanomethylene) Rhodanine as the Terminal Groups for Poly(3-Hexylthiophene)-Based Organic Solar Cells. *J. ACS Appl. Mater. Interfaces*, **2018**, *10*(40), 34427-34434, DOI: 10.1021/acsami.8b10312.

[20] Saha, P.; Karmakar P.; Deb, D., Modeling and simulation of P3HT and PCBM based organic optoelectronics devices. *Mater. Today: Proceedings*, **2020**, *43*, 3438-3442, DOI: 10.1016/j.matpr.2020.09.080.

[21] Hernandez, J. E.; Ahn, H.; Whitten, J. E., X-Ray and Electron Induced Oligomerization of Condensed 3-Hexylthiophene. *J. Phys. Chem.* B, **2001**, *105*, 8339-8344, DOI: 10.1021/jp010314o.

[22] Kolb, B.; Lentz, L. C.; Kolpak, A. M., Discovering Charge Density Functionals and Structure-property Relationships with PROPhet: A General Framework for Coupling Machine Learning and First-principles Methods. *Scientific Reports*, **2017**, *7*(1), 1-9, DOI: 10.1038/s41598-017-01251-z.

[23] Aboulouard, A.; Elhadadi, B.; Bensemlali, M.; Nasrellah, H.; Aarfane, A.; El idrissi, M., First-Principles Study on Optoelectronic Properties of New Quinacridone dye Derivatives in dye Sensitized Photovoltaic Cells. *Materials Today: Proceedings*, **2022**, *5*(317), DOI: 10.1016/j.matpr.2022.05.317.

[24] Mehboob, M. Y.; Hussain, R.; Adnan, M.; Saira, Farwa, U.; Irshad, Z.; Janjua, M. R. S. A., Theoretical Modelling of Novel Indandione-Based Donor Molecules for Organic Solar Cell Applications. *J. Physics and Chemistry of Solids*, **2022**, *152*, 110508, DOI: 10.1016/j.jpcsk.2021.110508.

[25] Mehboob, M. Y.; Hussain, R.; Khan, M. U.; Adnan, M.; Ehsan, M. A.; Rehman, A.; Janjua, M. R. S. A., Quantum Chemical Design of Near-infrared Sensitive Fused Ring Electron Acceptors Containing Selenophene as π-Bridge for High-performance Organic Solar Cells. *J. Phys. Org. Chem.*, **2021**, *34*(8), DOI: 10.1002/poc.4204.

[26] Khan, M. U.; Hussain, R.; Mehboob, M. Y.; Khalid, M.; Ehsan, M. A.; Rehman, A.; Janjua, M. R. S. A., First Theoretical Framework of Z-Shaped Acceptor Materials with Fused-Chrysene Core for High Performance Organic Solar Cells. *Spectrochimica Acta Part A: Molecular and Biomolecular Spectroscopy*, **2020**, Vol. ?, 118938, DOI: 10.1016/j.saa.2020.118938

[27] Mehboob, M. Y.; Hussain, R.; Asif Iqbal, M. M.; Irshad, Z.; Adnan, M., First Principle Theoretical Designing of W-shaped Dithienosilole-based Acceptor Materials Having Efficient Photovoltaic Properties for High-performance Organic Solar Cells. *Journal of Physics and Chemistry of Solids*, **2021**, *157*, 110202. DOI: 10.1016/j.jpcs.2021.110202

[28] Frisch, M. J. T.; Schlegel, G. W.; Scuseria, H. B.; Robb, G. E.; Cheeseman, M. A.; Scalmani, J. R.; Barone, G.; Mennucci, V.; Petersson, B.; Nakatsuji. G. A., vol. Revision D. 01. Wallingford CT: Gaussian. Inc., **2009**.

[29] Becke, A. D., Density-functional Exchange-energy Approximation with Correct Asymptotic Behavior. *Phys. Rev. A*, **1988**, *38*(6), 3098-100, DOI: 10.1103/PhysRevA.38.3098.

[30] Francl, M. M.; Pietro, W. J.; Hehre, W. J.; Binkley, J. S.; Gordon, M. S.; DeFrees, D. J.; Pople J. A., Self-consistent Molecular Orbital Methods. XXIII. A Polarization-type Basis Set for Second-row Elements. *J. Chem. Phys.*, **1982**, *77*(7), 3654-65, DOI: 10.1063/1.444267.

[31] Ahmed, S.; Kalita, D. J., Charge Transport in Isoindigo-dithiophene Pyrrole Based DA Type Oligomers: A DFT/TD-DFT Study for the Fabrication of Fullerene-Free Organic Solar Cells. *J. Chem. Phys.*, **2018**, *149*(23), 234906, DOI: 10.1063/1.5055306.

[32] Sahu, H.; Panda, A. N., Computational Investigation of Charge Injection and Transport Properties of a Series of Thiophene-pyrrole-based Oligo-azomethines. *Phys. Chem. Chem. Phys.*, **2014**, *16*(18), 8563-8574, DOI: 10.1039/C3CP55243H.

[33] Khan, M. U.; Iqbal, J.; Khalid, M.; Hussain, R.; Braga, A. A. C.; Hussain, M.; Muhammad, S., Designing Triazatruxene-based Donor Materials with Promising Photovoltaic Parameters for Organic Solar Cells. *RSC Adv.*, **2019**, *9*(45), 26402-26418, DOI: 10.1039/C9RA03856F.

[34] Zhu, C.; Guo, S.; Wang, P.; Xing, L.; Fang, Y.; Zhai, Y.; Dong, S., One-pot, Water-phase Approach to High-Quality Graphene/TiO_2 Composite Nanosheets. *Chem. Commun.*, **2010**, *46*(38), 7148-7150, DOI: 10.1039/C0CC01459A.

[35] OAldosari, O. F.; Iqbal, S.; Miedziak, P. J.; Brett, G. L.; Jones, D. R.; Liu, X.; Hutchings, G. J., Pd-Ru/TiO_2 Catalyst-an Active and Selective Catalyst for Furfural Hydrogenation. *Catalysis Science &Technology*, **2016**, *6*(1), 234-242, DOI: 10.1039/C5CY01650A.

[36] Kolev, T. M.; Yancheva, D. Y.; Stamboliyska, B. A.; Dimitrov, M. D.; Wortmann, R., Nonlinear Optical Properties of Pyridinium-betaines of Squaric Acid: Experimental and Theoretical Study. *Chem. Phys.*, **2008**, *348*(1-3), 45-52, DOI: 10.1016/ j.chemphys.2008.02.018.

[37] Bonaccorsi, R.; Scrocco, E.; Tomasi, J., The Properties of the Metal Complex Hydrides. *Theoreticachimicaacta*, **1979**, *52*(2), 113-127. DOI: 10.1007/BF00634787.

[38] Luque, F. J.; López, J. M.; Orozco, M., Perspective on Electrostatic Interactions of a Solute with a Continuum. A Direct Utilization of *Ab Initio* Molecular Potentials for the Prevision of Solvent Effects. *Theor. Chem. Acc.,* **2000**, *103*(3), 343-345, DOI: 10.1007/s002149900013.

[39] Sıdır; I., Density Functional Theory Design D-D-A Type Small Molecule with 1.03eV Narrow Band Gap: Effect of Electron Donor Unit for Organic Photovoltaic Solar Cell. *Mol. Phys.*, **2017**, *115*(19), 2451-2459, DOI: 10.1080/00268976.2017.1322722.

[40] Hurst, G. J.; Dupuis, M.; Clementi E., *Ab Initio* Analytic Polarizability, First and Second Hyperpolarizabilities of Large Conjugated Organic Molecules: Applications to Polyenes C_4H_6 to $C_{22}H_{24}$. *J. Chem. Phys.*, **2000**, *89*, 385-95, DOI: 10.1063/1.455480.

[41] Ansary, I.; Das, A.; Gupta, P. S.; Bandyopadhyay, A. K., Synthesis, Molecular Modeling of N-acyl Benzoazetinones and their Docking Simulation on Fungal Modeled target. *Synth Commun.*, **2017**, *47*, 1375-1386, DOI: 10.1080/00397911.2017.1328514.

[42] Chen, L.; Lu, J.; Huang, T.; Cai Y. D., A Computational Method for the Identification of Candidate Drugs for Non-small Cell Lung Cancer. *PLoS One*, **2017**, *12*, e0183411, DOI: 10.1371/journal.pone.0183411.

[43] Obot, I. B.; Obi-Egbedi, N. O.; Umoren, S. A., Antifungal Drugs as Corrosion Inhibitors for Aluminium in 0.1 M HCl. *Corrosion Sci.*, **2009**, *51*(8), 1868-75. DOI: 10.1016/ j.corsci.2009.05.017.

[44] Xue, Y.; Li, Z. R.; Yap, C. W.; Sun, L. Z.; Chen, X.; Chen. Y. Z., Effect of Molecular Descriptor Feature Selection in Support Vector Machine Classification of Pharmacokinetic and Toxicological Properties of Chemical Agents. *J. Chem. Inf. Comput. Sci.*, **2004**, *44*, 1630-8, DOI: 10.1021/ci049869h.

[45] Zhang, C.; Song, Y. L.; Wang, X., Correlations Between Molecular Structures and Third-order Non-Linear Optical Functions of Heterothmetallic Clusters: a Comparative Study. *Chem. Rev.*, **2007**, *251*, 1-2, DOI: 10.1016/j.ccr.2006.06.007.

[46] Gültekin, Z.; Demircioğlu, Z.; Frey, W.; Büyükgüngör, O., A Combined Experimental (XRD, FT-IR, UV-Vis and NMR) and Theoretical (NBO, NLO, Local & Global Chemical Activity) Studies of Methyl 2-((3R,4R)-3-(naphthalen-1-yl)-4-(phenylsulfonyl) isoxazolidin-2-yl) Acetate. *J. Mol. Struct.*, **2019**, *1199*, 126970, DOI: 10.1016/j.molstruc.2019.126970.

[47] Aboulouard, A.; Mtougui, S.; Demir, N.; Demir, N.; Moubarik, A.; El idrissi, M.; Can, M., New Non-Fullerene Electron Acceptors-based on Quinoxaline Derivatives Fororganic Photovoltaic Cells: DFT Computational Study. *Synth. Met.*, **2021**, Vol. ?, 116846, DOI: 10.1016/j.synthmet.2021.116846.